Journal of Building Engineering 26 (2019) 100921

Contents lists available at ScienceDirect

Journal of Building Engineering

journal homepage: http://www.elsevier.com/locate/jobe

Damage assessment of squat, thin and lightly-reinforced concrete walls by the Park & Ang damage index

Julian Carrillo [a,*], Claudio Oyarzo-Vera [b], Carlos Blandón [c]

[a] Department of Civil Engineering, Universidad Militar Nueva Granada, UMNG, Bogotá, Colombia
[b] Department of Civil Engineering, Universidad Católica de la Santísima Concepción, UCSC, Concepción, Chile
[c] Department of Civil Engineering, Universidad EIA, Medellín, Colombia

ARTICLE INFO

Keywords:
Damage index
Concrete wall
Thin wall
Squat wall
Crack pattern

ABSTRACT

Damage progression indexes are widely used to evaluate the performance of structural elements in buildings and bridges subjected to seismic actions. Although the Park & Ang damage index is currently implemented in several computational tools, the index has not been calibrated for squat and thin reinforced concrete (RC) elements controlled by shear deformations. It has been observed that the equations originally proposed for the Park & Ang damage index are unsuited for these types of structural elements, which are characterized by a failure mode dominated by shear instead of flexural deformations. The index was evaluated in this study for squat, thin and lightly-reinforced concrete walls using experimental data from a program comprising monotonic and reversed-cyclic load testing of 25 RC squat cantilever walls. The experimental program included walls, with and without openings, having height-to-length ratios equal to 0.5, 1.0 and 2.0. Full-scale wall thickness and clear height were 100 mm and 2.4 m, respectively. The specimens were built using three different types of concrete (normal-weight, light-weight and self-consolidating) with nominal compressive strength of 15 MPa. A novel formulation for the parameter β included in the Park & Ang damage index was proposed in this study using key variables of the wall specimens such as web reinforcement ratio and cumulative ductility. Comparison between the computed damage index and crack pattern evolution observed in wall specimens at different damage states demonstrated the ability of the model to numerically assess the damage of the wall specimens. Hence, this new formulation proposed for parameter β leads to a better estimation of damage for this particular type of elements when applying the broadly used Park & Ang damage index.

1. Introduction

Several structural response parameters can be associated with damage, such as drift, permanent deformations and energy dissipated by hysteresis. The challenge for the structural analysts is to detect and characterize the severity of damage and to determine the remaining capacity of the structure before reaching the failure condition. To achieve this in an effective way, it is deemed necessary to define threshold for the maximum or cumulative values of these parameters, and provide mechanical conditions that guarantee an optimal structural performance within these predefined limits. Damage index (*DI*) is a concept introduced for assessing damage in a quantitative manner. It consists on mathematical functions based on several structural parameters that quantify the structural damage in a scale varying between 0 and 1; zero for the no damage condition and one for the structural failure state [1].

In the case of reinforced concrete (RC), parameters such as non-recoverable deformations, displacement ductility and energy dissipated by hysteresis are generally considered as suitable damage parameters to introduce in these damage index functions [2].

Damage indexes have been used for more than 40 years [1–8]. One of the most widely used *DI* is the formulation proposed by Park & Ang [3, 4]. The index was conceived to quantify the structural damage for slender elements (beams or columns) that generally fail by flexural deformations. There is, however, a large inventory of buildings conformed by squat structural elements (walls), which failure mode is dominated by shear deformations and parameters for the Park & Ang *DI* (DI_{PA}) have not been calibrated. In particular, due to economic reasons, a large percentage of recent low- and medium-rise (up to four-story height) residential buildings in some countries in Latin America consists of RC walls with thickness smaller than 150 mm and only one center layer of

* Corresponding author.
E-mail addresses: wjcarrillo@gmail.com (J. Carrillo), coyarzov@ucsc.cl (C. Oyarzo-Vera), carlos.blandon@eia.edu.co (C. Blandón).

https://doi.org/10.1016/j.jobe.2019.100921
Received 18 December 2018; Received in revised form 8 August 2019; Accepted 12 August 2019
Available online 14 August 2019

Table 1
The Park & Ang damage index for different states of damage.

DI_{PA}	Observed damage
0.00–0.10	No damage - Localized minor cracking
0.10–0.25	Light damage - Minor cracking throughout.
0.25–0.40	Moderate damage - Severe cracking and localized spalling.
0.40–0.80	Severe damage - Crushing of concrete and exposure of reinforcing bars.
>0.80	Failure - Total failure of the structure.

web reinforcement.

Previous studies have investigated the capability of the DI_{PA} in assessing damage on squat elements (walls) showing that current parameters are not well suited to make accurate estimations for this type of structures [7,8]. Previous experimental programs have provided information about the seismic behavior of low aspect ratio reinforced concrete thin walls [9–14], and there are some studies aimed at evaluating its seismic performance in terms of damage. For instance, Carrillo and Alcocer [14] utilized a damage index based on the relation between the damaged area (area of cracks) and the area of the façade of the RC wall. Carrillo [6] proposed a damage index based on the stiffness degradation of walls. Such index depends on the story-drift ratio and the number of cycles experienced by the wall during a particular seismic event. Carrillo et al. [5] proposed a damage index to estimate the damage level and the residual performance based on the fractal dimension of the cracking recorded after an earthquake. Although damage index formulated by Park & Ang [3,4] is currently implemented in several computational tools, the index has not been calibrated for squat and thin elements controlled by shear deformations. Thereby, to improve the estimation of damage for squat, thin and lightly-reinforced concrete walls when applying the broadly used Park & Ang damage index, a novel formulation for the parameter β included in the Park & Ang damage index is proposed in this study. This novel equation is based on the experimental results obtained from quasi-static monotonic and reversed-cyclic test performed on 25 reinforced concrete walls. Damage of walls was initially assessed using the original formulation of Park & Ang [3,4]. Regression analyses were then performed for parameter β considering some of the variables originally considered by Park & Ang. Finally, the computed damage index was compared with the crack pattern evolution observed in typical walls at three different damage states.

2. The Park & Ang index

The original formulation proposed by Park & Ang [3,4] consists of a linear combination of the damage caused by excessive post-elastic deformations and the energy dissipated by the hysteresis or repeated cyclic loading effect of the element, as shown in Eq. (1).

$$DI_{PA} = \frac{u_{max}}{u_{mon}} + \beta \frac{E_H}{F_y \cdot u_{mon}} \quad (1)$$

where u_{max} is the ultimate deformation recorded on the element due to reversed-cyclic loading, u_{mon} is the ultimate deformation recorded on the element for monotonic loading, E_H is the total energy dissipated by hysteresis cycles, F_y is the yield strength of the element, and β is a non-negative parameter. Based on experimental data, the mentioned authors defined that the non-negative parameter β for slender elements is a function of the confinement ratio (ρ_w), the shear span ratio (l/d), the longitudinal reinforcement ratio (ρ_t) and the normalized axial force (n_0), as presented in Eq. (2).

$$\beta = 0.7^{\rho_w}\left(-0.447 + 0.073\frac{\ell}{d} + 0.24 n_0 + 0.314\rho_t\right) \quad (2)$$

The variables are limited to the following values: ρ_w varying between 0.2% and 2.0%, l/d between 1.0 and 6.6, n_0 between 0 and 0.52, ρ_w between 0.04% and 0.45%, and f'_c between 16 and 41 MPa. In addition, the variables must be considered as $l/d = 1.7$ when $l/d < 1.7$, $n_0 = 0.2$ when $n_0 < 0.2$ and $\rho_t = 0.75\%$ when $\rho_t < 0.75\%$. Table 1 shows the values of DI_{PA} reported by further investigations [15,16]. As shown in the table, these values are associated to different damage states.

Stephens and Yao [17] proposed a modified version for DI_{PA} to incorporate the effect of cumulative plastic deformations. These authors used this modified approach to assess the structural damage in a numerical model of a reinforced concrete frame structure tested under seismic actions. In this way, the DI_{PA} obtained from this numerical analysis was compared with the damage observed during seismic testing. The damage estimation obtained by the numerical model was consistent with the localized damage observed in the columns located at

Table 2
Main characteristics of wall specimens.

No.	Wall specimen	h_w mm	t_w mm	l_w mm	h_w/l_w	Type of concrete, f_c' MPa	Type of web reinf., f_y, MPa	Web reinf. % (ρ_w)	Boundary reinf. % (ρ_l)	Type of testing
3	MCN100 M	2417	101	2402	1.01	N, 18.8	D, 447	0.28	0.98	M
5	MCL50 M	2427	102	2397	1.01	L, 16.3	D, 447	0.14	0.68	M
6	MCL100 M	2425	101	2398	1.01	L, 16.3	D, 447	0.28	0.98	M
8	MCS100 M	2424	102	2397	1.01	S, 19.4	D, 447	0.28	0.97	M
10	MCN100C	2432	101	2397	1.01	N, 17.5	D, 447	0.28	0.98	C
12	MCS100C	2426	103	2401	1.01	S, 22.0	D, 447	0.28	0.96	C
17	MRN100C	2433	100	5400	0.45	N, 16.2	D, 447	0.28	0.22	C
18	MEN100C	2435	100	1240	1.96	N, 16.2	D, 447	0.28	1.50	C
19	MRN50C	2425	100	5400	0.45	N, 16.2	D, 447	0.14	0.22	C
20	MEN50C	2421	100	1240	1.95	N, 16.2	D, 447	0.14	1.04	C
21	MRL100C	2423	101	5413	0.45	L, 5.2	D, 447	0.28	0.32	C
22	MRN50mC	2401	103	5396	0.44	N, 20.0	W, 605	0.12	0.22	C
23	MCN50mC	2396	103	2398	1.00	N, 20.0	W, 605	0.12	0.72	C
24	MEN50mC	2399	101	1239	1.94	N, 20.0	W, 605	0.12	0.96	C
25	MRL50mC	2419	106	5415	0.45	L, 5.2	W, 605	0.12	0.21	C
26	MCL50mC	2423	100	2403	1.01	L, 26.0	W, 605	0.12	0.74	C
27	MEL50mC	2435	100	1221	1.99	L, 26.0	W, 605	0.12	0.82	C
28	MVN100C	2397	110	3826	N/A	N, 16.0	D, 447	0.26	0.82	C
29	MVN50mC	2397	110	3826	N/A	N, 16.0	W, 605	0.11	0.74	C
30	MCN50C-2	2400	100	2398	1.00	N, 20.0	D, 447	0.14	0.71	C
31	MCS50C-2	2404	104	2402	1.00	S, 27.1	D, 447	0.14	0.71	C
32	MCL50C-2	2426	100	2441	0.99	L, 26.0	D, 447	0.14	0.73	C
33	MCL100C-2	2432	98	2407	1.01	L, 5.2	D, 447	0.29	1.01	C
34	MCN50mC-2	2404	102	2401	1.00	N, 8.9	W, 605	0.12	0.73	C
35	MRN50mC-2	2401	100	5400	0.44	N, 8.9	W, 605	0.13	0.22	C

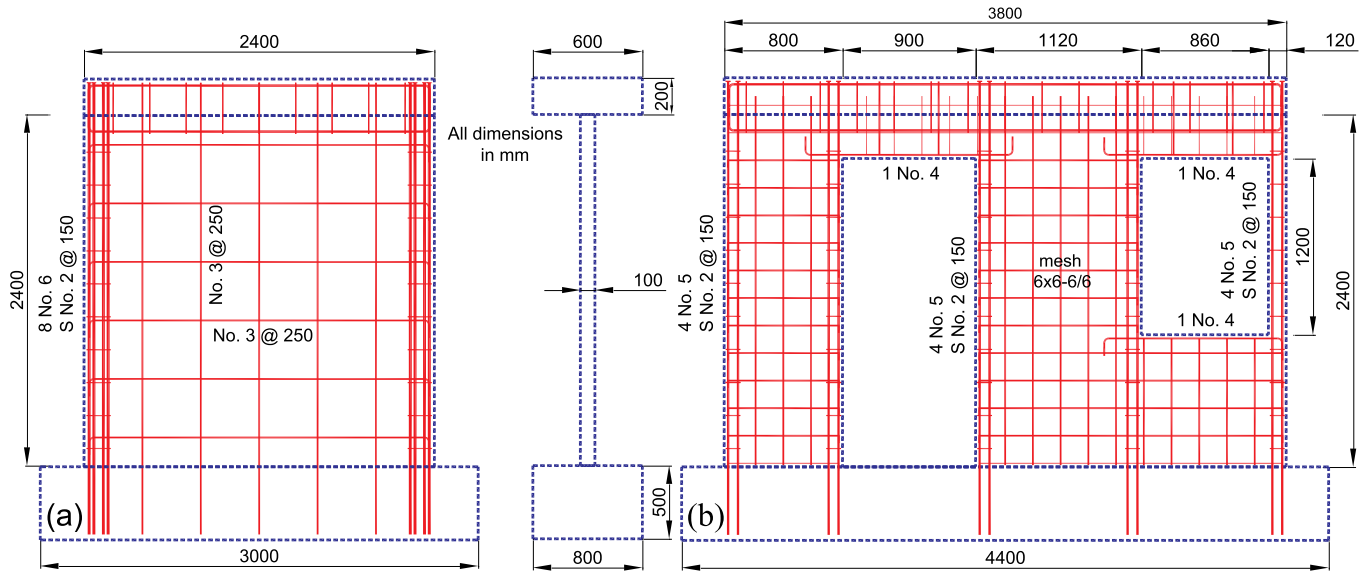

Fig. 1. Geometry and reinforcement layout of some wall specimens: (a) $h_w/l_w = 1.0$, 100% of ρ_{min} and using deformed bars; (b) wall with openings, 50% of ρ_{min} and welded-wire mesh.

the ground level.

Chai et al. [18] introduced the concept of plastic energy under monotonic loading to overcome the non-normalization obstacle in the index. This non-normalization obstacle is related to values of DI_{PA} greater than 1.0 when specimens are monotonically loaded to failure, due to the plastic energy dissipation under monotonic loading. Later on, Bozorgnia and Bertero [19] proposed a modification for DI_{PA} to solve the non-normalization issues by subtracting the elastic deformation from the maximum and ultimate deformation. More recently, Jiang et al. [20] proposed another variation of DI_{PA} to overcome the inconsistencies associated to non-normalization and identified correlations between parameter β and the confinement ratio, the shear span ratio and the axial load ratio. Oyarzo-Vera [8] assessed the damage of 12 reinforced concrete shear walls to integrate the concept of DI_{PA} to squat elements. The results of this research demonstrated that the parameter β proposed for flexural elements is not applicable to squat elements which behavior is governed by shear deformations.

3. Experimental program

The experimental program comprised monotonic (M) and reversed-cyclic (C) quasi-static load testing of 25 RC low aspect ratio cantilever walls. The main characteristics of 25 walls are summarized in Table 2. Typical geometry and reinforcement layout of some of the wall specimens are shown in Fig. 1. Reinforcement bar diameters are indicated in units of 1/8 of inch (e.g. No. 4 = 4/8"). Geometry and reinforcement layout of walls were designed to characterize reinforced concrete walls located at the first floor of typical two-story residential buildings in Latin America [9]. Characteristics of tested walls are distinctive of current design and construction practice for low-rise housing in several Latin American countries. Walls having height-to-length ratios (h_w/l_w) equal to 0.5 (R), 1.0 (C) and 2.0 (E), and walls with openings (V) simulating door and window openings were also tested in the experimental program. Full-scale wall thickness (t_w) and clear height (h_w) were 100 mm and 2.4 m, respectively. Then, to achieve the height-to-length ratio, length of walls was varied. Walls were built using three different types of concrete: normal-weight (N), light-weight (L) and self-consolidating (S). Nominal concrete compressive strength, f_c', was 15 MPa for all types of concrete. Ranges of measured mechanical properties of concrete for the 25 specimens are presented in Table 3. These properties were obtained at the time of testing walls. Thickness of boundary elements was equal to web thickness. To assess wall lateral shear strength, longitudinal boundary reinforcement was purposely designed to prevent flexural failure prior to achieving the typical shear failure observed in RC walls for low-rise housing. Aspect ratio and web steel ratio of walls were calculated from as built dimensions. A detailed description of the experimental program and design of the specimens is reported by Carrillo and Alcocer [9,10,12].

Three different web distributed reinforcement's ratios were considered: 100% of the minimum reinforcement's ratio ($\rho_{min} = 0.25\%$), 50% of ρ_{min} (0.125%), and without reinforcement (0% of ρ_{min}, for reference only). Carrillo and Alcocer [14] argued that, because of the large wall-to-floor area ratio and the high redundancy offered by this type of construction, web reinforcement could be reduced from the amount currently required for walls (0.25%) when two conditions are fulfilled: (i) shear demand is less than one-half the concrete contribution to shear strength and, (ii) the house is located in low- and medium-hazard seismic zones where design is controlled by vertical actions, or by temperature effects on concrete.

Minimum web steel ratio (ρ_{min}) was that prescribed by ACI-318 [21] and was placed in a single layer at mid-thickness of the wall in both direction using the same ratios of horizontal and vertical reinforcement ($\rho_h = \rho_v$). Web shear reinforcement was provided either by deformed bars (D) or welded-wire meshes made of small-gage wires (W). Nominal yield strength of deformed bars and wire reinforcement, f_y, was 412 MPa (for mild steel) and 491 MPa (for cold-drawn wires). The ranges of

Table 3
Measured mechanical properties of concrete.

Property	Normal-weight (N)	Light-weight (L)	Self-consolidating (S)
Compressive Strength, f'_c, MPa	16.0–24.7	10.8–26.0	22.0–27.1
Young's Modulus, E_c, MPa	8430–14750	6700–10790	8900–11780
Specific dry weight, γ, kN/m^3	18.8–20.3	15.2–18.3	18.9

Table 4
Measured mechanical properties of reinforcement.

Location in the wall	Boundary reinforcement	Web reinforcement: deformed bar (D)	Web reinforcement: welded wire (W)
Type	Mild	Mild	Cold-drawn
Yield strength, f_y, MPa	411–456	435–447	605–630
Ultimate strength, f_u, MPa	656–721	659–672	687–700
Elongation, %	9.1–16.0	10.1–11.0	1.4–1.9

measured mechanical properties of steel reinforcement for the 25 specimens are presented in Table 4. The cold-drawn wire reinforcement used in this study did not exhibit a significant plastic plateau as low-carbon bars show. The elongation capacity (at fracture) of the small diameter wires was much shorter than that of mild-steel reinforcement. The behavior of wire reinforcement was characterized by fracture of material at very low values elongation [12].

Walls were tested under quasi-static (monotonic and reversed-cyclic) load testing. For the monotonic load test, an incremental unidirectional quasi-static lateral load was applied at the top of the wall. Monotonic test was finished when 80% decrement of the maximal load was observed. In the case of reversed-cyclic load test, the loading protocol consisted of a series of increasing amplitude cycles. The load history is presented in Fig. 2. The initial loading cycles were applied to reach the 85% of the theoretical cracking load, followed by cycles that increases the precedent load in 50%. This loading history was repeated up to diagonal cracking due to shear was observed. After that, test loading was controlled by drift, applying increments of 0.2%. For each increment, two cycles at same amplitude were applied [11]. An axial compressive stress of 0.25 MPa was applied on top of the walls and kept constant during testing procedure. This stress corresponded to an average axial load in the first floor walls of a two-story prototype house.

For evaluating the observed wall behavior, three failure modes were defined as follows: a) when yielding of more than 75% of the web shear reinforcement and no web crushing of concrete was observed, a diagonal tension failure (DT) was defined; b) when yielding of more than 50% of steel bars or wires, and web crushing and spalling of concrete was observed, a diagonal compression failure (DC) was defined, and, c) when yielding of more than 75% of the web steel reinforcement and web crushing of concrete was observed, a mixed failure mode (DT-DC) was defined. Walls reinforced with 50% of the minimum code prescribed web steel reinforcement ratio and using deformed bars or welded-wire mesh, exhibited DT failure. Failure mode was governed by web inclined cracking of concrete at approximately 45-degree angle and yielding of most of web shear reinforcement prior to severe strength and stiffness decay. In walls reinforced with welded-wire meshes, fracture of wires after plastic yielding of web shear reinforcement was observed. Failure was brittle because of the limited elongation capacity of the wire mesh itself (see Table 4). In contrast, walls reinforced using deformed bars and minimum web steel ratio exhibited DT-DC failure.

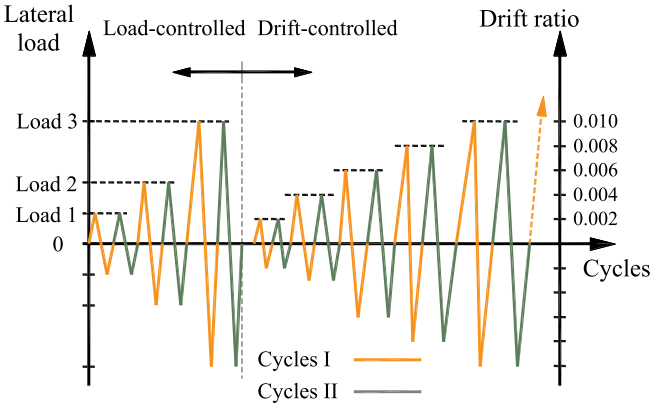

Fig. 2. Loading protocol history applied during quasi-static cyclic tests.

4. Damage assessment of walls using the Park & Ang index

In this study, the damage of walls was initially assessed using the original formulation of Park & Ang [3,4]. The parameters considered by Park & Ang in Eq. (1) were the ultimate deformation recorded on the element for reversed-cyclic loading (u_{max}), ultimate deformation registered on element for monotonic loading (u_{mon}), yield strength of the element (F_y) and the total energy dissipated by hysteresis cycles (E_H).

Most structures have some capacity for deformation beyond the peak of the strength-deformation relation with some reduction in strength. It should be reasonable to recognize at least part of this post-peak deformation capacity. Therefore, a rational definition for post-peak displacement is the displacement recorded when the load carrying capacity has undergone a small reduction, i.e. 20% or 25% [22]. Correspondingly with previous studies [9,14], the ultimate deformation observed in wall specimens during reversed-cyclic loading (u_{max}) was calculated applying the criteria of 20% of strength degradation. That is, u_{max} is related to the displacement recorded during the hysteresis cycle that evidenced a 20% of strength decay (δ_{uc}) compared to the maximum strength recorded during the reversed-cyclic loading test [9,14]. The ultimate deformation registered on the specimen during monotonic loading (u_{mon}) was not available for all the specimens included in the experimental program, because not all cyclic tests were accompanied by monotonic tests. Hence, this variable was estimated in this study from the envelope of the hysteresis curves recorded for each of the walls. The ultimate deformation related to monotonic test was assimilated to the ultimate deformation taken from the envelope curve of the measured hysteresis cycles (δ_{um}), applying the aforementioned 20% strength degradation criterion. Results for both monotonic and cyclic tests were available for walls MCS100, MCL100, MCN100 and MCL50 [24]. Based on those results, it was estimated that δ_{um} was 1.3 times larger than the ultimate deformation recorded on the envelope curve of the hysteresis cycles (δ_{uce}). Hence, δ_{um} was used in Eq. (1) instead of u_{mon} to calculate

Table 5
Variable considered for the calculation of DI_{PA} [24].

No.	Wall specimen	δ_{uc} mm	δ_{um} mm	F_y kN	E_H kN-mm
10	MCN100C	35.9	51.3	375	47769
12	MCS100C	40.1	56.1	374	45552
17	MRN100C	20.2	28.7	589	27245
18	MEN100C	45.2	61.9	168	25820
19	MRN50C	24.8	36.0	525	35261
20	MEN50C	53.7	70.1	127	20294
21	MRL100C	30.2	43.2	651	57092
22	MRN50mC	10.0	16.1	624	13567
23	MCN50mC	11.5	19.0	256	4287
24	MEN50mC	14.5	24.3	122	1984
25	MRL50mC	10.0	15.7	475	6935
26	MCL50mC	14.7	21.5	328	11110
27	MEL50mC	17.9	26.0	129	3090
28	MVN100C	29.8	45.7	129	23628
29	MVN50mC	10.3	16.6	155	5143
30	MCN50C-2	19.9	31.1	258	12329
31	MCS50C-2	18.2	23.8	256	10114
32	MCL50C-2	30.2	42.6	290	35715
33	MCL100C-2	40.1	52.2	247	37545
34	MCNB50mC	11.2	15.1	196	1865
35	MRNB50mC	18.9	24.7	466	21765

Table 6
Parameterβ calculated using the original formulation of Park & Ang [3,4].

No.	Wall specimen	ρ_w, %	h_w/l_w	ρ_l, %	n_0	β_{T1}	β_{T2}	β_{exp}
10	MCN100C	0.28	1.0	0.98	0.02	−0.056	0.030	0.121
12	MCA100C	0.28	1.0	0.96	0.02	−0.061	0.024	0.131
17	MRN100C	0.28	1.0	0.22	0.02	−0.272	−0.036	0.184
18	MEN100C	0.28	2.0	1.50	0.02	0.158	0.197	0.109
19	MRN50C	0.14	0.5	0.22	0.02	−0.320	−0.037	0.167
20	MEN50C	0.14	2.0	1.04	0.02	0.029	0.070	0.103
21	MRL100C	0.28	0.5	0.32	0.02	−0.276	−0.036	0.148
22	MRN50mC	0.12	0.5	0.22	0.02	−0.323	−0.038	0.281
23	MCN50mC	0.12	1.0	0.72	0.02	−0.137	−0.038	0.448
24	MEN50mC	0.12	2.0	0.96	0.02	0.005	0.046	0.603
25	MRL50mC	0.12	0.5	0.21	0.02	−0.326	−0.038	0.390
26	MCL50mC	0.12	1.0	0.74	0.02	−0.131	−0.038	0.201
27	MEL50mC	0.12	2.0	0.99	0.02	0.014	0.055	0.338
28	MVN100C	0.26	0.63	0.96	0.02	−0.086	0.024	0.087
29	MVN50mC	0.11	0.63	0.96	0.02	−0.091	0.026	0.190
30	MCN50C-2	0.14	1.0	0.74	0.02	−0.130	−0.037	0.234
31	MCA50C-2	0.14	1.0	0.71	0.02	−0.139	−0.037	0.142
32	MCL50C-2	0.14	1.0	0.73	0.02	−0.133	−0.037	0.101
33	MCL100C-2	0.29	1.0	1.01	0.02	−0.047	0.038	0.080
34	MCNB50mC	0.12	1.0	0.73	0.02	−0.134	−0.038	0.410
35	MRNB50mC	0.13	0.5	0.22	0.02	−0.321	−0.038	0.124

DI_{PA}.

The definition of yielding often causes difficulty since the strength-deformation relation may not have a well-defined yield point. For squat reinforced concrete walls, the displacement corresponding to the development of 75% or 80% of the maximum strength usually, though not necessarily, is close to the point of first significant yield [23]. Since yielding of longitudinal bars in squat reinforced concrete walls is not observed in the same way than in columns, the yield strength of the squat element (F_y) was considered as 80% of the maximum strength recorded in the wall [9,14]. Finally, the total energy dissipated by hysteresis cycles (E_H) corresponded to the sum of all areas encircled by the hysteresis cycles during the entire reversed-cyclic test until the ultimate state condition related to the 20% strength degradation criterion was observed. The results of all these parameters for each of the walls under analysis are presented in Table 5.

4.1. Calculation of parameter β based on the theoretical formula

The β parameter was computed considering the formula presented in Eq. (2), using the data presented in Table 2. The parameters considered in Eq. (2) were the confinement ratio (ρ_w), shear span ratio (l/d), longitudinal reinforcement ratio (ρ_t) and normalized axial force (n_0). In this study, parameters ρ_w, l/d and ρ_t were assimilated to the transversal reinforcement ratio (ρ_w), aspect ratio (h_w/l_w) and reinforcement ratio at boundary elements (ρ_l), respectively. It is worth noting that Park & Ang established conditions for these variables previously presented in Section 2 that were not satisfied by the specimens under study. For example, the lower limit of transversal reinforcement ratio (ρ_w) in the original Park & Ang formulation is 0.2%. However, 14 walls under examination did not fulfill this condition. The minimum aspect ratio (h_w/l_w) accepted by the original model is 1.0, and 6 walls had aspect ratios close to 0.5. Reinforcement ratio at boundary elements (ρ_l) always exceeded the upper limit stablished by the model (ρ_l<0.45%) because the longitudinal reinforcement at boundary elements of these walls were designed to avoid a flexural failure. Finally, the normalized axial force (n_0) applied to all walls in this study was smaller than the minimum value considered by Park & Ang, as the walls were representative of low-rise buildings.

The results of β calculations considering the theoretical formula proposed in Eq. (2) are presented in Table 6. In this table, the parameter β_{T1} symbolizes the theoretical value of β taking into account the exact value of the model variables (ρ_w, h_w/l_w, ρ_l and n_0) and β_{T2} denotes the theoretical value of β considering the limits of the variables established by the original model. It is observed in Table 6 that parameters β_{T1} and β_{T2} adopted negative values in several cases. This was inconsistent with Park & Ang formulation, because it means that the reversed cycles of loading did not have an accumulative damage effect. Hence, the formulation proposed for β by Park & Ang in Eq. (2) cannot be directly utilized for squat elements.

Table 7
Values adopted by parameter β_{exp}.

Type of web reinforcement	Min	Max	Mean
Deformed bars	0.08	0.23	0.13
Welded-wire mesh	0.12	0.60	0.33

Table 8
Damage index calculated using the formulation of Park & Ang [3,4].

No.	Wall specimen	β_{T2}	DI_{PA}	Contribution of plastic deformation	Contribution of cumulative effect of cycles
10	MCN100C	0.030	0.774	90%	10%
12	MCA100C	0.024	0.767	93%	7%
18	MEN100C	0.197	1.220	60%	40%
20	MEN50C	0.070	0.926	83%	17%
24	MEN50mC	0.046	0.628	95%	5%
27	MEL50mC	0.055	0.740	93%	7%
28	MVN100C	0.024	0.749	87%	13%
29	MVN50mC	0.026	0.671	92%	8%
33	MCL100C-2 (14)	0.038	0.879	87%	13%

4.2. Estimation of parameter β based on damage observations

Considering that all wall specimens reached the ultimate failure condition, the damage index should be equal to 1 for all the cases. Therefore, an experimental value for parameter β can be calculated by clearing it from Eq. (1) as shown in Eq. (3), and using the information available in Table 5. The results of this calculation is presented in the last column of Table 6 as β_{exp}.

$$\boldsymbol{\beta_{exp}} = \left(1 - \frac{\boldsymbol{\delta_{uc}}}{\boldsymbol{\delta_{um}}}\right) \frac{\boldsymbol{F_y \delta_{um}}}{\boldsymbol{E_H}} \quad (3)$$

The values adopted by β_{exp} show a large dispersion ranging from 0.08 to 0.60. However, as shown in Table 7, different values of β_{exp} were observed for walls with web shear reinforcement made of deformed bars

Table 9
Variables considered relevant to calculate β in squat and thin walls.

No.	Wall specimen	ρ_w %	h_w/l_w	μ_{cum}	β_{exp}
10	MCN100C	0.28	1.0	96.3	0.12
12	MCA100C	0.28	1.0	43.1	0.13
17	MRN100C	0.28	1.0	17.2	0.18
18	MEN100C	0.28	2.0	46.6	0.11
19	MRN50C	0.14	0.5	58.0	0.17
20	MEN50C	0.14	2.0	79.3	0.10
21	MRL100C	0.28	0.5	67.7	0.15
22	MRN50mC	0.12	0.5	27.1	0.28
23	MCN50mC	0.12	1.0	18.5	0.45
24	MEN50mC	0.12	2.0	10.6	0.60
25	MRL50mC	0.12	0.5	7.4	0.39
26	MCL50mC	0.12	1.0	13.9	0.20
27	MEL50mC	0.12	2.0	14.0	0.34
28	MVN100C	0.26	0.63	73.0	0.09
29	MVN50mC	0.11	0.63	40.5	0.19
30	MCN50C-2 (9)	0.14	1.0	105.8	0.23
31	MCA50C-2(11)	0.14	1.0	129.8	0.14
32	MCL50C-2(13)	0.14	1.0	96.8	0.10
33	MCL100C-2 (14)	0.29	1.0	61.7	0.08
34	MCNB50mC	0.12	1.0	9.2	0.41
35	MRNB50mC	0.13	0.5	32.5	0.12

and for walls with welded-wire mesh. Several authors [16,17,25] propose values of β close to 0.15 for elements with stable hysteresis cycles like those observed in walls reinforced with deformed bars, and values of β higher than 0.2 for elements that exhibits significant strength degradation, which can be the case of walls reinforced with welded-wire mesh. Results presented in Table 7 for the walls included in the study reported herein were slightly different to those reported in previous studies [16,17,25], especially for walls reinforced with welded-wire mesh.

4.3. Calculation of the damage index using theoretical formulas

Even though the drawback of having negative theoretical values for β, damage assessment using the original formulation of Park & Ang was attempted for the case of those walls that has a non-negative value for parameter β_{T2}. The results of this analysis is presented in Table 8. It is observed in the table that, in all the cases, DI_{PA} exceeded the value of 0.4 which is assigned by Park et al. [15], and Williams and Sexsmith [16] as the lower limit for severe damage, but only in three cases, it exceeded the limit 0.8 which is assigned to failure condition. These results were not consistent with the damage observed in the walls as all of the specimens were tested up to failure. It is important to remark that the contribution to damage assigned to the cumulative effect of reversed-cyclic loads ($\beta E_H/F_y u_{mon} \approx 10\%$) was significantly lower than the contribution of the plastic deformations ($u_{max}/u_{mon} \approx 90\%$), as shown in the last two columns of Table 8.

4.4. Derivation of a novel formula for β

The main objective of this study was obtaining a novel formulation for computing the value of parameter β that characterizes the behavior of squat, thin and lightly-reinforced concrete walls. Initially, regression analyses were performed considering some of the variables originally considered by Park & Ang [3,4], i.e. aspect ratio (h_w/l_w) and web transversal reinforcement ratio (ρ_w); while others variables were excluded, such as type of concrete, longitudinal reinforcement (ρ_l) and normalized axial load (n_0). The type of concrete was excluded because it is not commonly used as a design parameter (type of concrete) for practical design. In addition, Carrillo et al. [13] reported that initial stiffness, hysteresis curves and energy dissipation of walls made of light-weight and normal-weight concrete was readily comparable. The two latter variables (ρ_l and n_0) were also excluded because they became less relevant in the dominant shear failure mode of these walls and less significant in the case of low-rise buildings; i.e. values of ρ_l and n_0 are low and almost constant for the prototype of low-rise house. In addition, cumulative ductility (μ_{cum}) was considered as a relevant variable to calculate β based on previous studies [7,8,26]. Cumulative ductility is a response parameter associated to the cumulative damage effect of reversed loading cycles. This parameter is defined [8] as the sum of the ductility demands that have exceeded the elastic limit as presented in Eq. (4).

$$\mu_{cum} = \frac{\sum_{k=1}^{n} \delta_k}{\delta_y} \tag{4}$$

where δ_y is the deformation at the top of the wall at flexural yield condition, and δ_k is the maximum plastic deformation at the top of the wall for cycle k that is computed using Eq. (5). As explained previously, since the flexural yield condition was not observed in the squat reinforced concrete walls, δ_y was associated to the yield strength F_y that was computed as 80% of the maximum strength recorded in the wall.

$$\boldsymbol{\delta_k} = \begin{cases} \mathbf{0 when \delta_k < \delta_y} \\ \mathbf{or} \\ \mathbf{\delta_k when \delta_k > \delta_y} \end{cases} \tag{5}$$

The values adopted by parameters ρ_w, h_w/l_w and μ_{cum} in each wall are presented in Table 9. The correlation between these parameters and β_{exp} is showed in Fig. 3. It can be observed in the figure that parameters ρ_w and μ_{cum} can be correlated to β_{exp} using a power function, while in the case of parameter h_w/l_w, the highest correlation was achieved by a linear regression. The relatively low correlation coefficient with parameter β_{exp} achieved by parameter ρ_w ($r = 0.62$) and h_w/l_w ($r = 0.22$) is explained by the scarce diversity of values of those parameters in the tested walls. Such lacking data hinder the possibility of finding a better representation of the influence of these parameters in damage progression of wall specimens. On the other hand, the highest correlation coefficient

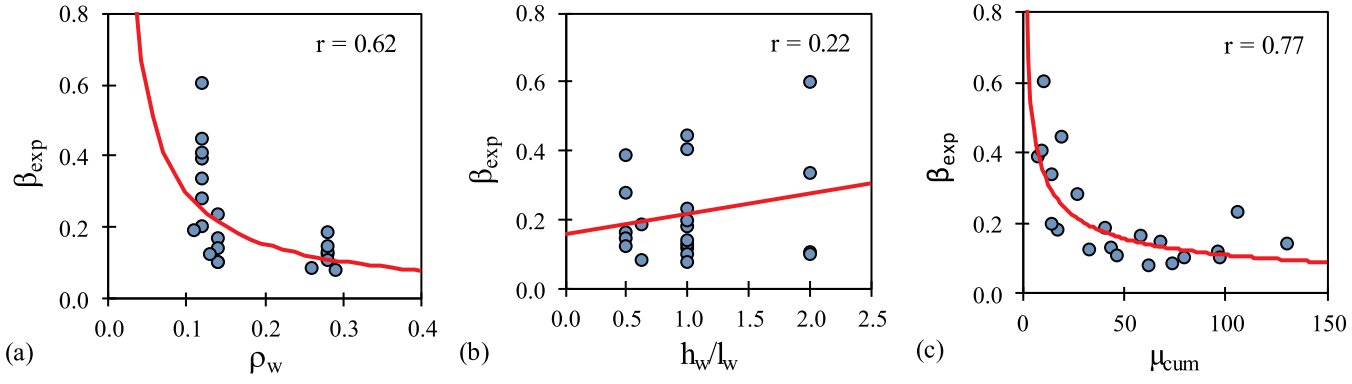

Fig. 3. Correlations between parameter β_{exp} and parameters: (a) ρ_w, (b) h_w/l_w, (c) μ_{cum}.

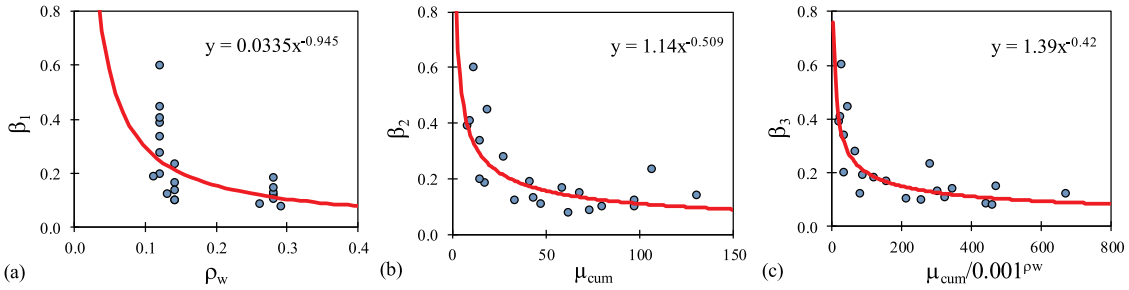

Fig. 4. Adjusted curve for: (a) model β_1, (b) model β_2, (c) model β_3.

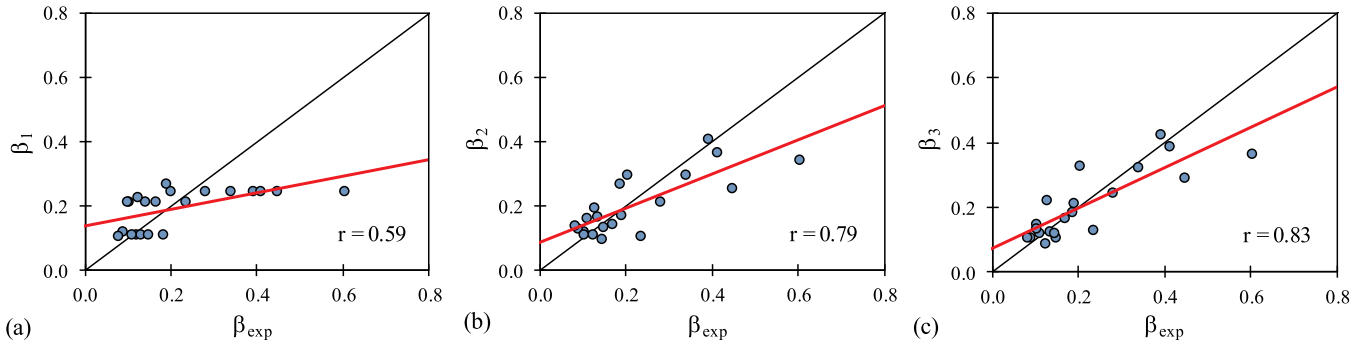

Fig. 5. Comparison between: (a) β_{exp} and model β_1, (b) β_{exp} and model β_2, (c) β_{exp} and model β_3.

($r = 0.77$) was obtained when the influence of μ_{cum} was analyzed. This correlation between μ_{cum} and β_{exp} was expected, because μ_{cum} is a variable that directly evinced the importance of the cumulative effect of reversed loading cycles in damage of structural elements.

Based on results showed in Fig. 3, parameters μ_{cum} and ρ_w were selected in this study as key parameters to develop a novel mathematical function to calculate β in the case of squat, thin and lightly-reinforced concrete walls. This scatter in Fig. 3b is related to walls with significant different characteristics (type and steel ratio of web reinforcement) and the same value of aspect ratio. According to non-dimensional analyzes, three different regression analysis were develop to compute β. Two of them corresponded to a power function that considered one single parameters – ρ_w in the case of Eq. (6) and μ_{cum} in the case of Eq. (7). The third model represented in Eq. (8) was found by the authors as the model with the highest correlation for combining both parameters ρ_w and μ_{cum}. In that case, parameters were determined based on a sensitivity analysis and by non-linear iterative regression analysis with the aim of obtaining the highest correlation between β_3 and β_{exp}. Graphical representations of these models are presented in Fig. 4.

$$\beta_1 = 0.0335 \times \rho_w^{-0.945} \tag{6}$$

$$\beta_2 = 1.14 \times \mu_{cum}^{-0.509} \tag{7}$$

$$\beta_3 = 1.39 \times \left(\frac{\mu_{cum}}{0.001^{\rho_w}}\right)^{-0.42} \tag{8}$$

In the case of β_1 and β_2, the models generally underestimate parameter β and exhibited correlation coefficients (r) relative to β_{exp} equal to 0.59 and 0.79, respectively (Fig. 5a and b). In the case of β_3, the model underestimate parameter β mainly for walls with low ductility capacity that resulted in large values for β_{exp} (for example; walls with web shear reinforcement made of welded-wire meshes MCN50mC and MEN50mC). The model exhibited correlations coefficients relative β_{exp} higher than the coefficients associated to other two models ($r = 0.83$), as presented in Fig. 5c. Consequently, the suitable model proposed in this study for computing β of squat, thin and lightly-reinforced concrete walls is β_3 as defined in Eq. (8).

4.5. Damage assessment using the updated formulation for DI_{PA}

After defining the novel proposal for calculating parameter β presented in Eq. (8), it is possible to assess damage using the Index proposed by Park & Ang (Eq. (1)). This was made on a group of 6 typical walls part of the experimental set tested for this study. Two walls were selected for each aspect ratio (h_w/l_w) with different web reinforcement ratios (ρ_w) and different type of web reinforcement (deformed bars or welded-wire mesh).

Three damage states (DS) were identified during the testing of each wall according to the limit states classification proposed by Carrillo and Alcocer [14]. Such classification defines three limit states: diagonal cracking (DS1), maximum or peak lateral resistance (DS2), and loss of lateral resistance (DS3). Diagonal cracking (DS1) was defined as the drift corresponding to the onset of inclined web cracking. This limit state is sometimes called inclined shear cracking. Peak lateral resistance (DS2) was defined as the drift corresponding to the maximum lateral strength of the walls. Loss of lateral resistance (DS3) was defined as the drift corresponding to a decrease in peak lateral resistance of 20% in any direction of loading during the seismic event. Damage index was calculated for these walls at each of these damage states using the equations proposed in the study reported herein (Eqs. (1) and (8)). The results for these walls are shown in Table 10, along with the damage severity scale presented in Table 1.

As shown in Table 10, DI_{PA} adopted values similar to 1.0 at DS3 for 5 of the 6 wall specimens. These results were anticipated because the model for parameter β was calibrated in this study considering this failure condition ($DI_{PA} = 1$). However, the computed value of DI_{PA} exceeded the maximum limit (1.0) for the wall MCL50mC, that corresponded to a wall with low ductility capacity associated to the type of web shear reinforcement (welded-wire mesh). Only in one case DI_{PA} was lower than 0.9, but still in the range of failure condition ($DI_{PA} > 0.8$).

For DS2 limit state, the values of DI_{PA} ranged from 0.4 to 0.8 for 4 of the 6 wall specimens. These values are associated to severe damage that coincide with the condition observed on tested walls at this state of damage; i.e. concrete crushing and reinforcement exposure due to concrete spalling. The other 2 walls exceeded the upper limit for severe

Table 10
The Park & Ang damage index (DI_{PA}) for different damage states of walls.

Wall specimen	h_w/l_w	ρ_w %	Type of Reinf.	Damage state	δ_{uc} mm	δ_{um} mm	E_H kN-mm	F_y kN	β_3	DI_{PA}	Damage classification (see Table 1)
MCA100C	1.00	0.28	D	DS1	15.0	56.1	3620	374	0.128	0.29	Moderate
				DS2	25.3		18013			0.56	Severe
				DS3	40.0		45552			0.99	Failure
MCL50mC	1.00	0.12	M	DS1	5.0	21.5	1281	328	0.327	0.29	Moderate
				DS2	15.1		9306			1.13	Failure
				DS3	14.7		11110			1.20	Failure
MRN100C	0.45	0.28	D	DS1	6.4	28.7	6743	589	0.188	0.30	Moderate
				DS2	15.1		14365			0.68	Severe
				DS3	20.2		27245			1.00	Failure
MRN50mC	0.45	0.12	W	DS1	2.1	16.1	1249	624	0.239	0.16	Light
				DS2	10.0		12644			0.92	Failure
				DS3	9.7		13567			0.92	Failure
MEN100C	1.95	0.28	D	DS1	8.6	61.9	820	168	0.128	0.15	Light
				DS2	35.1		10524			0.70	Severe
				DS3	45.1		21782			1.00	Failure
MEN50mC	1.95	0.12	W	DS1	7.9	24.3	426	122	0.380	0.38	Moderate
				DS2	14.5		1391			0.77	Severe
				DS3	14.3		1984			0.84	Failure

damage ($DI_{PA} > 0.8$) and incur in the range of structural failure. Finally, computed values of DI_{PA} were always smaller than 0.4 at DS1. These lower DI_{PA} values at DS1 were attributed to moderate and light damage, and coincide with lower levels of cracking observed on wall specimens. Fig. 6 shows the damage evolution of typical specimens. In the figure, shrinkage cracks are displayed using blue lines. As shown in Fig. 6, all these results are consistent with the damage patterns observed in the walls.

5. Conclusions

Damage progression on squat, thin and lightly-reinforced concrete walls tested under monotonic and cyclic load up to failure were evaluated in this study. The Park & Ang damage index was utilized to assess damage on these specimens. It was found that the equation originally proposed by Park & Ang (1985) to calculate parameter β (Eq. (2)) in slender elements was not suitable to be used for squat, thin and lightly-reinforced concrete walls, because its failure mode was dominated by shear instead of flexural deformations. For most of the wall specimens, parameter β calculated as suggested by Park & Ang, resulted in negative values and, consequently, it was not possible to calculate the damage index.

To fill this gap in the literature, parameter β was experimentally calculated in this study from the hysteretic response of 25 wall specimens. A strong correlation was identified between parameter β and key variables of the wall specimens such as web reinforcement ratio (ρ_w) and cumulative ductility (μ_{cum}). This strong correlation confirmed the results previously reported for squat reinforced concrete elements. The correlation proposed in this study is described by a power regression. Comparison between the computed damage index and crack pattern evolution observed in the walls at different damage states demonstrated the ability of the model to numerically assess the damage of the wall specimens for different performance levels when applying the Park & Ang damage index. The proposed equation results in a novel formulation

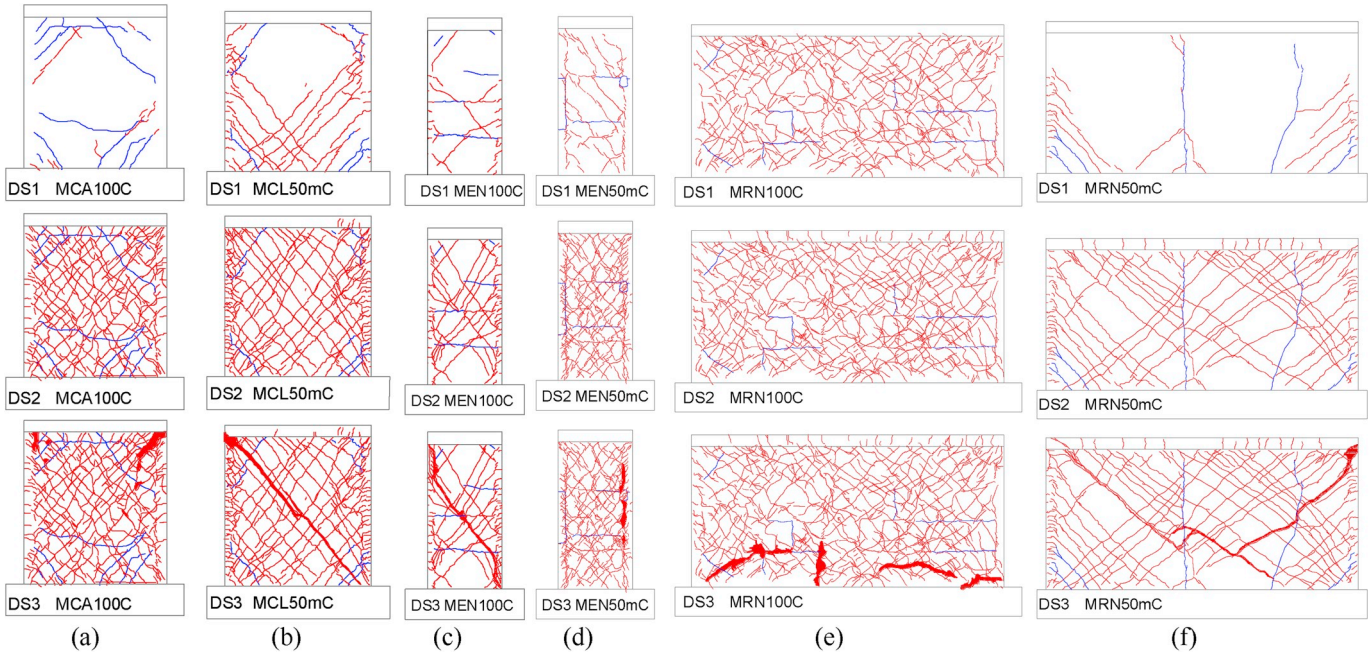

Fig. 6. Damage evolution of typical specimens: (a) MCA100C, (b) MCL50mC, (c) MEN100C, (d) MEN50mC (e) MRN100C, (f) MRN50mC.

of parameter β (Eq. (8)) to be used for squat, thin and lightly-reinforced concrete structural elements, such as the walls tested in this experiment.

Acknowledgements

The authors gratefully acknowledge Vicerrectoría de Investigaciones at the Universidad Militar Nueva Granada (UMNG, Colombia) for financing the research project INV-ING-2743. The authors also recognize the assistance from Kevin González during numerical processing. The views expressed in this paper are solely those of the authors and do not necessarily reflects the views of the sponsor.

References

[1] V. Bertero, B. Bresler, Developing methodologies for evaluating the earthquake safety of existing buildings, in: Report No. UCB/EERC-77-06, University of California, Berkeley, 1971.
[2] Banon, D. Veneziano, Seismic safety of reinforced concrete members and structures, Earthq. Eng. Struct. Dyn. 10 (2) (1982) 179–193.
[3] Y. Park, A. Ang, Mechanistic seismic damage model for reinforced concrete, Journal of Structural Engineering, ASCE 111 (4) (1985) 722–739, https://doi.org/10.1061/(ASCE)0733-9445 (1985) 111:4(722).
[4] Y. Park, A. Ang, Y. Wen, Seismic damage analysis of reinforced concrete buildings, Journal of Structural Engineering, ASCE 111 (4) (1985) 740–757, https://doi.org/10.1061/(ASCE)0733-9445 (1985) 111:4(740).
[5] J. Carrillo, D. Dominguez, N. Prado, Seismic damage index based on fractal dimension of cracking on thin reinforced concrete walls, ACI Struct. J. 114 (6) (2017) 1649–1658, https://doi.org/10.14359/51700919.
[6] J. Carrillo, Damage index based on stiffness degradation of low-rise RC walls, Earthq. Eng. Struct. Dyn. 44 (6) (2015) 831–848, https://doi.org/10.1002/eqe.2488.
[7] C. Oyarzo-Vera, Assessment of damage of low slenderness reinforced concrete walls using the damage index of Park & Ang, Obras y Proyectos 1 (2005) 23–26 (in Spanish).
[8] C. Oyarzo-Vera, Damage evaluation in r/c shear walls using the damage index of Park & Ang, in: Proceedings of the First European Conference on Earthquake Engineering and Seismology, 2006 (Geneva, Switzerland).
[9] J. Carrillo, S. Alcocer, Backbone model for performance-based seismic design of RC walls for low-rise housing, Earthq. Spectra 28 (3) (2012) 943–964, https://doi.org/10.1193/1.4000068.
[10] J. Carrillo, S. Alcocer, Seismic performance of concrete walls for housing subjected to shaking table excitations, Eng. Struct. 41 (2012) 98–107, https://doi.org/10.1016/j.engstruct.2012.03.025.
[11] J. Carrillo, S. Alcocer, Experimental investigation on dynamic and quasi-static behavior of low-rise reinforced concrete walls, Earthq. Eng. Struct. Dyn. 42 (5) (2013) 635–652, https://doi.org/10.1002/eqe.2234.
[12] J. Carrillo, S. Alcocer, Shear strength of reinforced concrete walls for seismic design of low-rise housing, ACI Struct. J. 110 (3) (2013) 415–425, https://doi.org/10.14359/51685599.
[13] J. Carrillo, J. Lizarazo, R. Bonett, Effect of lightweight and low-strength concrete on seismic performance of thin and lightly-reinforce shear walls, Eng. Struct. 93 (2015) 61–69, https://doi.org/10.1016/j.engstruct.2015.03.022.
[14] J. Carrillo, S. Alcocer, Acceptance limits for performance-based seismic design of RC walls for low-rise housing, Earthq. Eng. Struct. Dyn. 41 (15) (2012) 2273–2288, https://doi.org/10.1002/eqe.2186.
[15] Y. Park, A. Ang, Y. Wen, Damage-limiting aseismic design of buildings, Earthq. Spectra 3 (1) (1987) 1–26, https://doi.org/10.1193/1.1585416.
[16] M. Williams, R. Sexsmith, Seismic damage indices for concrete structures: a state-of-the-art review, Earthq. Spectra 11 (2) (1995) 319–349, https://doi.org/10.1193/1.1585817.
[17] J. Stephens, J. Yao, Damage assessment using response measurements, Journal of structural Engineering, ASCE 113 (4) (1987) 787–801, 10.1061/(ASCE)0733-9445 (1987)113:4(787).
[18] Y. Chai, K. Romstad, S. Bird, Energy-based linear damage model for high-intensity seismic loading, Journal of Structural Engineering, ASCE 121 (5) (1995) 857–864, https://doi.org/10.1061/(ASCE)0733-9445 (1995)121:5(857).
[19] Y. Bozorgnia, V. Bertero, Damage spectra: characteristics and applications to seismic risk reduction, Journal of Structural Engineering, ASCE 129 (10) (2003) 1330–1340, https://doi.org/10.1061/(asce)0733-9445 (2003)129:10(1330).
[20] H.J. Jiang, B. Fu, X.L. Lu, L.Z. Chen, Seismic damage assessment of RC members by a modified Park & Ang model, Adv. Struct. Eng. 18 (3) (2015) 353–364, https://doi.org/10.1260/1369-4332.18.3.353.
[21] ACI Committee 318, Building Code Requirements for Structural Concrete and Commentary, American Concrete Institute, *ACI*, Farmington Hills, USA, 2014.
[22] R. Park, Ductility evaluation from laboratory and analytical testing, in: Proceedings of the 9th World Conference on Earthquake Engineering – 9WCEE vol. 8, 1988, pp. 605–616. Tokyo, Japan.
[23] T. Salonikios, A. Kappos, I. Tegos, G. Penelis, Cyclic load behavior of low-slenderness reinforced concrete walls: failure modes, strength and deformation analysis, and design implications, ACI Struct. J. 97 (1) (2000) 132–142.
[24] K. González, Evaluation of the Park & Ang Damage Index for Concrete Walls of Social Welfare Housing, Bachelor Thesis, Civil Engineering, Nueva Granada Military University, UMNG, Colombia, 2016 (In Spanish).
[25] E. Cosenza, G. Manfredi, Damage indices and damage measures, Prog. Struct. Eng. Mater. 2 (1) (2000) 50–59.
[26] F. Carrasco, M. Behrens, C. Oyarzo-Vera, Effects of duration of earthquakes on the inelastic response of structures, Obras y Proyectos 7 (2010) 54–60 (in Spanish).